On the Numerical Reconstruction of Images from a Microwave Hologram

KEINOSUKE NAGAI, YOSHINAO AOKI, AND MICHIO SUZUKI

Abstract—A new technique for the numerical reconstruction of images from a long-wavelength hologram is proposed. The technique is to calculate images by the fast Fourier transform (FFT) algorithm with the hologram data sampled by a straight line approximation. This sampling technique is convenient to reduce the number of the sampling points, and the image can be reconstructed with less data than the conventional equally spaced sampling method. A one-dimensional hologram is constructed at S band and an image is reconstructed by the proposed method. These results are discussed and compared with the results of the conventional numerical reconstruction.

I. Introduction

IN THE PROCESS of reconstructing images from microwave or soundwave holograms, the optical method is usually adopted for its ease and high capacity as a processor. The numerical method using a computer is another technique for hologram data processing. The disadvantage of the numerical method is that the hologram information to be processed by this method is greatly limited by practical considerations compared with the optical method. However, since the information contained in a microwave or soundwave hologram is much less than that of an optical hologram, the numerical method is a promising technique in reconstructing images from long-wavelength holograms. A few papers have reported on this technique [1]–[3]. In these papers, the hologram data are sampled at equally spaced sampling points and two-dimensional Fresnel transform of the sampled data is calculated using the fast Fourier transform (FFT) algorithm [4], resulting in the reconstruction of images. In this paper a straight line approximation technique is proposed to sample the hologram data and a method to insert dummy data is discussed to apply the FFT algorithm in the proposed sampling technique. Since this technique has the advantage that images can be calculated with less nonzero data, compared with the conventional sampling technique, it is useful in situations where the total number of the sampling points of the hologram is limited. To verify the proposed technique, a one-dimensional microwave hologram is recorded at S band. This one-dimensional hologram is sampled with the straight line approximation and an image is calculated. The results obtained are discussed and compared with those of the conventional numerical reconstruction method.

II. Sampling of Hologram Data

A. Equally Spaced Sampling

In scanned-type holography, it takes much time to construct a hologram. To overcome this disadvantage, a linear or planar detecting array system can be considered. In this system the number of array elements is limited from the technical and economical points of view. Therefore, it is questioned how to arrange the array elements on the hologram plane. The most suitable way is to place them at equally spaced points, when any information of hologram data is not known *a priori*. The same situation occurs in the numerical image reconstruction, where the FFT algorithm is used, resulting in the sampling at equally spaced points. This sampling method determines a criterion for the maximum spatial frequency to be recorded as the hologram data.

Let the number of the equally spaced sampling points be N with respect to the one-dimensional hologram of aperture L. The spacing Δx of each sampling point is obtained as follows:

$$\Delta x = \frac{L}{N} . \tag{1}$$

Since the hologram aperture is limited, the higher spatial-frequency part of the hologram cannot be recorded. The maximum spatial frequency $f_{A\max}$ to be recorded in the hologram is obtained referring to the result of [6]:

$$f_{A\max} = \frac{L}{2\lambda z_1} \tag{2}$$

where λ is the wavelength of the microwave signal and z_1 is the distance from the object plane to the hologram plane. On the other hand, the maximum spatial frequency $f_{S\max}$ allowable for the sampling with the period Δx is obtained by the sampling theory as follows:

$$f_{S\max} = \frac{1}{2\Delta x} . \tag{3}$$

Therefore, the maximum frequency $f_{\max}$ of the hologram is determined as the lower one of $f_{A\max}$ and $f_{S\max}$ and is expressed as follows:

$$f_{\max} = \min (f_{A\max}, f_{S\max}). \tag{4}$$

Roughly speaking, the resolution of the reconstructed images depends on the value of $f_{\max}$. This fact suggests to us that the most desirable way for arranging sampling points on the hologram plane is to place them as satisfying the following condition:

$$f_{A\max} = f_{S\max}. \tag{5}$$

From (1)–(3), the minimum spacing $(\Delta x)_{\min}$ and the aperture L to satisfy (5) are obtained with the parameters λ, z_1, and N:

$$(\Delta x)_{\min} = \frac{\lambda z_1}{L} = \left(\frac{\lambda z_1}{N}\right)^{1/2} \tag{6}$$

$$L = (\lambda z_1 N)^{1/2}. \tag{7}$$

Manuscript received February 7, 1972; revised August 14, 1972.

The authors are with the Department of Electronic Engineering, Hokkaido University, Sapporo, Japan.

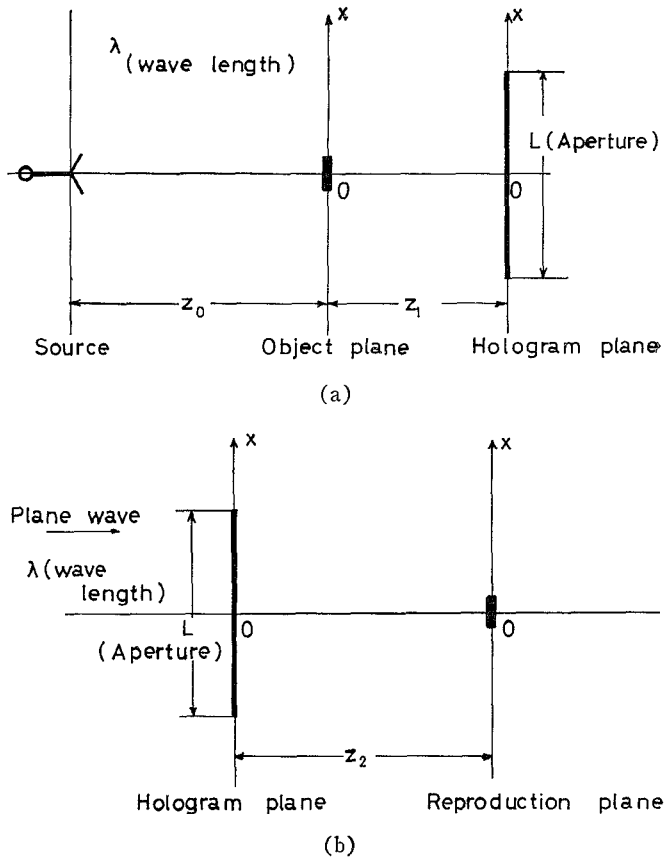

Fig. 1. The geometry of the problem. (a) The geometry of producing the hologram. (b) The optical geometry of reproducing images.

Thus the maximum frequency is as follows:

$$f_{\max} = \frac{1}{2}\left(\frac{N}{\lambda z_1}\right)^{1/2}. \tag{8}$$

Equation (8) expresses the criterion for the resolution of the reconstructed images.

B. Reduction of Sampling Points

For a given sampling number N, the minimum spacing $(\Delta x)_{\min}$ is determined by (6). When a hologram of a point object, that is a Fresnel zone plate, is considered, $(\Delta x)_{\min}$ is the spacing between two zones at the aperture end $x = L/2$ [see Fig. 1(a), letting $z_0 \to \infty$] with the paraxial ray approximation. The variance of the interference fringes of a zone plate becomes smaller as the center is approached. A hologram may be considered as a linear superposition of many zone plates [5]. For example, object waves O_1 and O_2 of two point objects are assumed to be recorded by the square-law detection with a coherent background b, and the hologram h is expressed as follows:

$$h = |b + O_1 + O_2|^2 = |b|^2 + b^*(O_1 + O_2) + b(O_1^* + O_2^*) + |O_1 + O_2|^2. \tag{9}$$

Since the background term b is assumed to be much greater than object terms O_1 and O_2, the term $|O_1+O_2|^2$ can be neglected and (9) expresses the linear superposition of object waves O_1 and O_2. Therefore, near both centers of the zone plates associated with object waves O_1 and O_2, the interference fringes vary slowly by virtue of the linear superposition, while they vary rapidly toward the edge of the aperture. These facts suggest the reduction of sampling points near the centers of the zone plates. For example, a zone plate may be sampled with the sampling period $2(\Delta x)_{\min}$, twice that of the minimum sampling period of (6), at the center part of the hologram, while with the sampling period $(\Delta x)_{\min}$ at another part, without greatly deteriorating the quality of reconstructed images. From these arguments, if the geometry of the object and illuminating waveshapes, that is the geometrical shadow of the object on the hologram plane, is known, it is possible to sample the hologram data with a greater sampling period than $(\Delta x)_{\min}$ at the shadow area, where the interference fringes vary slowly without much deterioration of the reconstructed images. In this manner the sampling points may be reduced as compared with the equally spaced sampling.

However, a problem arises when the hologram data of the reduced sampling points are processed numerically with the aid of the FFT algorithm. The FFT algorithm requires the sampled data at equally spaced points. To solve this problem, a technique to insert dummy data is considered. However, if the dummy data to be inserted in the calculation process are nonzero, the advantage of reducing the sampling points vanishes. For this reason, the hologram data are sampled with a straight line approximation, where dummy data can be transformed to zero-valued data in the stage of computation.

III. Algorithm of Fourier Transform by Straight Line Approximation

A. Fourier Transform by Straight Line Approximation

A brief explanation is presented to evaluate the Fourier transform by the straight line approximation. As shown in Fig. 2(a), a function $g(x)$ is approximated by a polygon $g_p(x)$ with only straight lines. Let $g_k = g(x_k)$ $(k = 0, 1, \cdots, N-1)$ be the value of $g(x)$ at the point x_k where $g(x_k) = g_p(x_k)$. The second-order derivative of $g_p(x)$ can be expressed as follows:

$$\frac{d^2 g_p(x)}{dx^2} = \sum_{k=1}^{N-2} g_k'' \delta(x - x_k) \tag{10}$$

where

$$g_k'' = g_k' - g_{k-1}' \tag{11}$$

$$g_k' = \frac{g_{k+1} - g_k}{x_{k+1} - x_k} \tag{12}$$

and $\delta(x)$ is the Dirac delta function. The schematic explanation to deduce (10)–(12) is shown in Fig. 2. Let $G(f)$ be the Fourier transform of the function $d^2g(x)/dx^2$ defined as follows:

$$G(f) = \int_{-\infty}^{\infty} \frac{d^2 g(x)}{dx^2} \exp\left[-j2\pi f x\right] dx. \tag{13}$$

Substituting (10) into (13), $G(f)$ can be expressed as follows [7]:

$$G(f) = \sum_{k=1}^{N-2} g_k'' \exp\left[-j2\pi f x_k\right]. \tag{14}$$

Equation (14) has a form similar to a discrete Fourier transform (DFT), but it differs from the DFT in the point that the

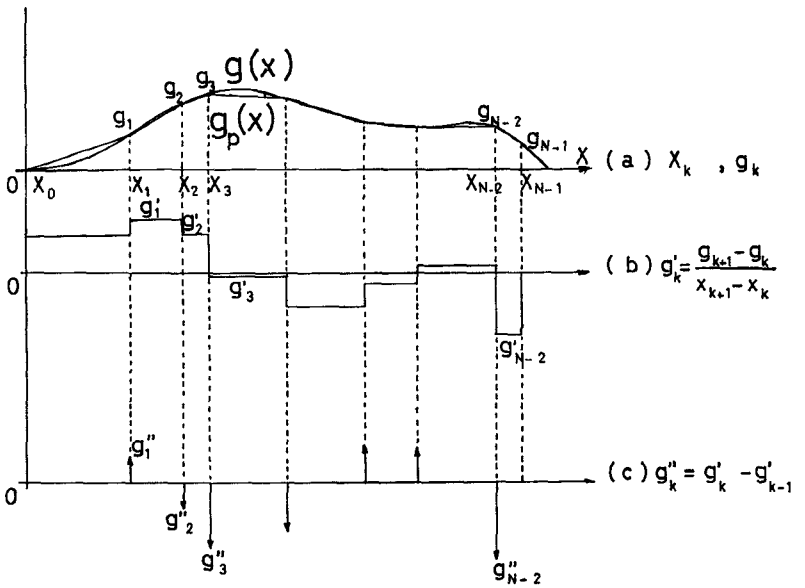

Fig. 2. The explanation of x_k, $g(x)$, $g_p(x)$, g_k, g_k', and g_k''.

sampling point x_k can be chosen arbitrarily in the straight line approximation, while the DFT requires the sampled data at equally spaced points. The arbitrariness of sampling is an advantage of the straight line approximation.

B. Application of FFT

In order to calculate $G(f)$ of (14) by the FFT algorithm, it is necessary to coincide (14) formally with the DFT. For this reason $g(x)$ is considered within the region $[0, L]$ and outside of this region $g(x)$ repeats itself with the period L. Therefore, the following relation is added:

$$g_N = g_0 \tag{15}$$

$$g_{N-1}' = \frac{g_N - g_{N-1}}{L - x_{N-1}} = g_{-1}' \tag{16}$$

and from (11),

$$g_0'' = g_0' - g_{-1}'$$

$$g_{N-1}'' = g_{N-1}' - g_{N-2}'. \tag{17}$$

Adding g_0'' and g_{N-1}'' to (14), the following expression can be obtained (see Fig. 2):

$$G(f) = \sum_{k=0}^{N-1} g_k'' \exp\left[-j2\pi f x_k\right]. \tag{18}$$

The region $[0, L]$ is assumed to be divided into N sections with equal spacing and the straight line approximation is adopted. Then x_k of (18) expresses the sampling coordinate at equally spaced points and is written as follows:

$$x_k = \frac{L}{N} k, \qquad k = 0, 1, \cdots, N-1. \tag{19}$$

In the DFT, the frequency is also sampled in the frequency domain as follows:

$$f = \frac{1}{L} r, \qquad r = 0, 1, \cdots, N-1. \tag{20}$$

Substituting (19) and (20) into (18),

$$G(r) = \sum_{k=0}^{N-1} g_k'' \exp\left[-j2\pi \frac{rk}{N}\right] \tag{21}$$

is obtained, where $G(r/L)$ is expressed by $G(r)$. Using (21), the Fourier spectrum $G(r)$ can be calculated with the data g_k'' obtained by the straight line approximation. However, in (21), the advantage that the arbitrary points can be chosen as the sampling points in (18) is lost. For this reason, a technique to insert the dummy data is proposed to save the advantage of the straight line approximation even a little.

C. Insertion of Dummy Data

In the smooth part of the original function $g(x)$, the straight segments of the polygon $g_p(x)$ can be taken longer than the minimum sampling period determined by a certain criterion. In the discussion on the zone plate in Section II-A, this criterion is the minimum sampling period $(\Delta x)_{\min}$ of (6) to record the maximum frequency $f_{\max}$ of (8). In Section II-B it is argued that the sampling points can be reduced near the center of the zone plate, where the function of the zone plate becomes smoother. For example, the smooth part of the function can be sampled with the period twice of the fundamental one as shown in Fig. 3. However, additional data, that is dummy data, are necessary to process the data by (21). If the dummy data to be inserted are nonzero data, it is useless to reduce sampling points at the smooth part of the function. Since the second-order derivative of the straight line is zero, the dummy data g_{k-1}'' at the unsampled point x_{k-1} are always zero, as shown in Fig. 3, in the straight line approximation:

$$g_{k-1}'' = 0. \tag{22}$$

With the data of (22), the number of calculating operations in the FFT algorithm can be reduced. If the total number of the sampling points is limited in the hologram-constructing system, the hologram can be sampled more closely at the part of fine interference fringes, or a larger hologram aperture can be recorded compared with the equally spaced sampling, inserting dummy data by the straight line approximation. The error of the FFT in the straight line approximation can be estimated by the deviation of the polygon from the original func-

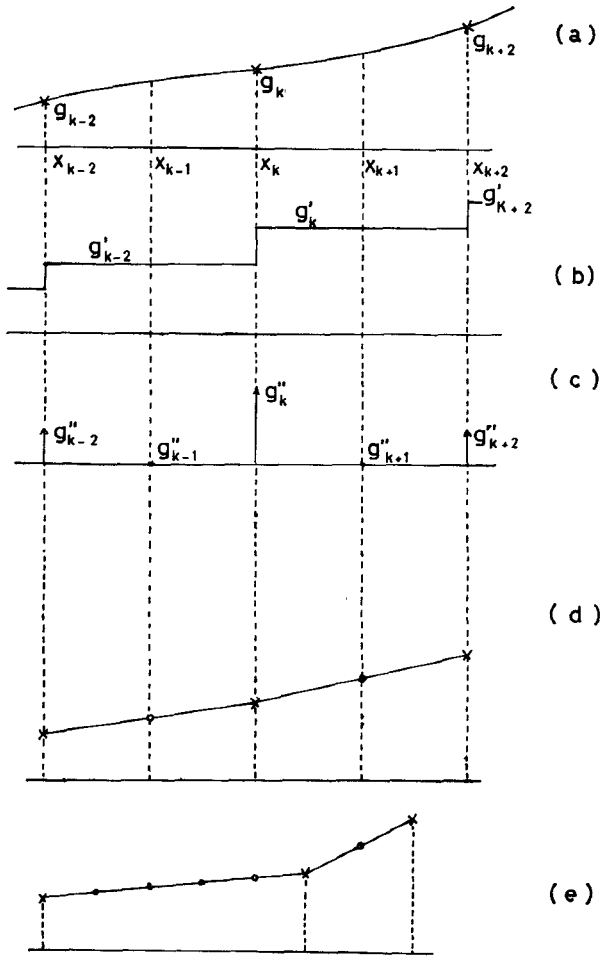

Fig. 3. Insertion of the dummy data and the reproduced data by the inverse transform. (a) Data g_{k-2}, g_k, and g_{k+2} exist only at x_{k-2}, x_k, and x_{k+2}, respectively. (b) g_k'. (c) g_k'' is nonzero at x_{k-2}, x_k, x_{k+2}, and zero at the other points. (d) Data by the inverse transform: - - - - - - - - - - o; original data: - - - ×. (e) The general case.

tion, while the error of the customary DFT is understood as the aliasing error.

D. Inverse Transform and Convolution

The orthogonal property of exponential function in the DFT guarantees the existence of the inverse discrete Fourier transform (IDFT). This fact means that the inverse transform of (21) can be found as follows:

$$g_k'' = \frac{1}{N}\sum_{r=0}^{N-1} G(r)\exp\left[j2\pi\frac{kr}{N}\right]. \tag{23}$$

The sampled value g_k of the original function can be calculated with the obtained value g_k'' of (23). Since g_k is assumed to be sampled at equally spaced points, the following relation can be derived from (12) and (15):

$$\sum_{k=0}^{N-1} g_k' = 0. \tag{24}$$

Similarly, from (11) and (16), the following relation is obtained:

$$\sum_{k=0}^{N-1} g_k'' = 0. \tag{25}$$

Assuming a trial value $g_0' = g_0' + \Delta g'$ of g_0', the first-order derivative g_k' can be calculated by (11) and (17) as follows:

$$g_k' = g_k'' + g_{k-1}' + \Delta g' \tag{26}$$

where $\Delta g'$ is the deviation of g_k' from the true value of g_k'. The deviation $\Delta g'$ can be obtained from (26) using (24) and (25):

$$\Delta g' = \frac{1}{N}\sum_{k=0}^{N-1} g_k'. \tag{27}$$

Once $\Delta g'$ is obtained, the true g_k' can be calculated successively from (26). The same discussion can be conducted to calculate g_k by (12) from the calculated g_k', where (28) is used instead of (24):

$$G_p(0) = \sum_{k=0}^{N-1} g_k \tag{28}$$

where $G_p(0)$ is the zero-frequency component of the Fourier spectrum of the polygon $g_p(x)$, that is, the area of the polygon. The inverse transform of (23) reproduces the unsampled value g_{k-1} corresponding to the dummy data $g_{k-1}''(=0)$ of (22) on the straight line, as shown in Fig. 3.

In the numerical reconstruction of the Fresnel transform hologram, the main subject is to calculate the convolution of the hologram and the propagation function. The convolution $q(x)$ of two functions $g_p(x)$ and $p(x)$ can be expressed by (29), taking account of the straight line approximation

$$\frac{d^2q(x)}{dx^2} = \frac{d^2g_p(x)}{dx^2} * p(x) \tag{29}$$

where the asterisk expresses the convolution integral. Let $G(f)$ and $P(f)$ be the Fourier transforms of $d^2g_p(x)/dx^2$ and $p(x)$, respectively. The second-order derivative q_k'' of $q(x)$ can be obtained to calculate the inverse Fourier transform of $G(r)\cdot P(r)$ according to (23). The procedure to calculate $q(x)$ from q_k'' is the same as to calculate g_k from g_k'' as mentioned before, where (30) is used instead of (28):

$$\sum_{k=0}^{N-1} q_k = Q(0) = G_p(0)\cdot P(0). \tag{30}$$

In (30), q_k are the sampled values of $q(x)$ at equally spaced points and $Q(0)$ is the zero-frequency component of the Fourier spectrum of the polygon made of q_k.

IV. Experiment

A. Construction of a One-Dimensional Hologram

A one-dimensional microwave hologram is recorded in the experimental configuration of Fig. 1(a). The frequency of the microwave signal is chosen as 9.4 GHz. The object is an aluminium plate of 20 cm width and 2 m length. A diode detector scans the microwave field along the horizontal line of about 2 m length, where the height of the line is arranged to be the same as that of the wave source. Thus the data of the one-dimensional hologram are obtained. The distance z_0 from the source plane to the object plane and z_1 from the object plane to the hologram plane are chosen as $z_0 = 4.8$ m and $z_1 = 1.8$ m, respectively. The hologram obtained is shown in

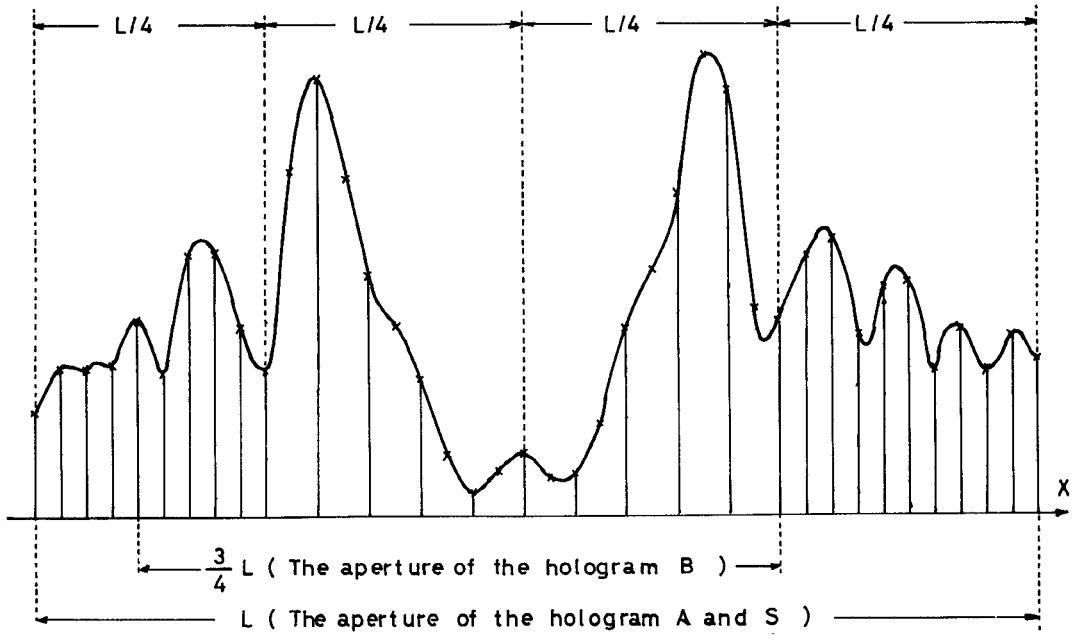

Fig. 4. Hologram. Sampling points: hologram A and B; ——×—— A (40) B (30): hologram S; longitudinal lines (30).

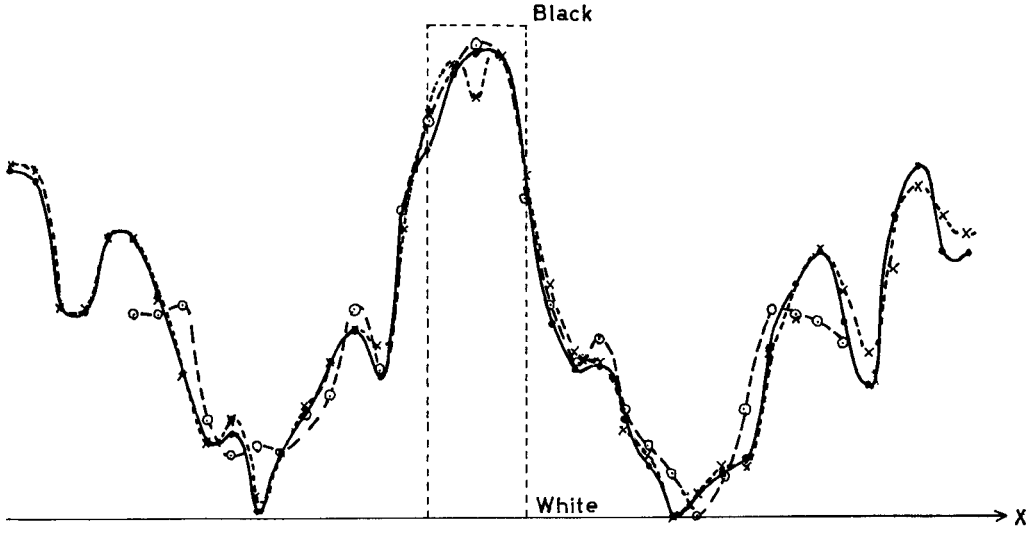

Fig. 5. The reconstructed images. ——●—— The image from the hologram A by the DFT. ---⊙--- The image from the hologram B by the DFT. --- ×--- The image from the hologram S by the only straight line approximation method.

Fig. 4, where the interference fringes become finer as the aperture edge is approached.

For the numerical reconstruction, this one-dimensional hologram is sampled in three ways. First, the hologram of the whole aperture L is sampled with 40 equally spaced sampling points; this is hologram A. The hologram of aperture $3L/4$ is sampled with the same sampling period as A and is named hologram B. This hologram consists of 30 sampling points. The hologram S is made for the straight line approximation method, where the hologram of aperture L is divided into four parts, that is, two center parts and two edge parts, and the hologram is sampled with 10 sampling points at center parts, with 20 sampling points at the edges. Thus the sampled data of hologram S coincide with those of hologram A at the edges, while they coincide with all other data of hologram A at the center parts. To process the data of hologram S, 10 dummy data points, that is 10 zeros, are inserted at the center parts, resulting in the data of 40 sampled points in the stage of computer calculation. These different ways of sampling are shown in Fig. 4.

B. Numerical Reconstruction of Images by Computer

Since the numerical reconstruction of images from long-wavelength holograms is described in detail in [3], the outline of the procedure is mentioned briefly. Refering to the optical reconstruction in the geometry of Fig. 1(b), where the optical wavelength is assumed to be same as that of the microwave and the hologram reduction process is neglected for simplicity

of discussion, the images are reconstructed to perform the Fresnel transform of the hologram, as expressed by the following convolution equation:

$$q(x) = h(x) * p(x) \tag{31}$$

where $q(x)$ and $h(x)$ express the reconstructed image and the hologram. The function $p(x)$ in (31) is called a propagation function and is expressed as follows:

$$p(x) = \exp\left(-j\frac{\pi}{\lambda z_2}x^2\right) \tag{32}$$

where z_2 is the distance between the hologram plane and the image plane as shown in Fig. 1(b). The position z_2 of the image plane can be determined as follows [3, eq. (6):]

$$z_2 = \frac{z_1(z_0 + z_1)}{z_0}. \tag{33}$$

The Fourier transform $P(f)$ of $p(x)$ can be calculated analytically as follows:

$$P(f) = \exp(j\pi\lambda z_2 f^2) \tag{34}$$

where the constant coefficient is neglected. Since the frequency domain is also sampled with the interval $1/L$ as shown in (20) in the FFT algorithm, (20) is substituted into (34), resulting in the following:

$$P\left(\frac{r}{L}\right) = \exp(j\pi z r^2) \tag{35}$$

where

$$z \equiv \frac{\lambda z_2}{L^2} = \frac{\lambda z_1(z_0 + z_1)}{L^2 z_0}. \tag{36}$$

The parameter z of (36) can be calculated with the experimental values of λ, L, z_0, and z_1 in the hologram-construction process.

The numerical reconstruction of images is conducted with respect to three holograms A, B, and S. The parameter z of (36) is calculated with the experimental values, resulting in $z=0.02$ [$z=0.02\times(4/3)^2$ in the case of B]. In practice, the best images are reconstructed for the value $z=0.0203$ [$z=0.0203\times(4/3)^2$ in the case of B]. The images from holograms A and B are numerically reconstructed according to the customary DFT algorithm, and the calculated images are shown in Fig. 5. A recognizable difference between these images suggests the effect of the number of sampling points and aperture sizes of holograms on the reconstructed images. The image from hologram S is also reconstructed by the straight line approximation method. The reconstructed image is shown in Fig. 5. This image closely resembles that of hologram A, especially at the edges where the image from hologram B has no reconstructed image points because of the shortage of sampling points. This means that the image reconstructed with 30 true data and 10 dummy (zero) data by the straight line approximation method is almost equivalent to the image reconstructed with 40 true data by the customary DFT method. This experimental result confirms the argument that the sampling points on the hologram can be reduced and images can be reconstructed numerically with less data by the straight line approximation, as compared with the customary DFT method. The numerical reconstruction by the straight line approximation has a potentiality in a holographic system where the hologram data are sampled with a limited number of detectors arranged on the hologram plane and the hologram data are processed by the computer of an on-line system to reconstruct images in real time without optical processing.

References

[1] J. W. Goodman and R. W. Lawrence, "Digital image formation from electronically detected holograms," *Appl. Phys. Lett.*, vol. 11, pp. 77–79, Aug. 1967.

[2] Y. Aoki and A. Boivin, "Computer reconstruction of images from a microwave hologram," *Proc. IEEE (Special Issue on Detection Theory and Applications)* (Lett.), vol. 58, pp. 821–822, May 1970.

[3] Y. Aoki, "Optical and numerical reconstruction of images from sound-wave holograms," *IEEE Trans. Audio Electroacoust.*, vol. AU-18, pp. 258–267, Sept. 1970.

[4] W. T. Cochran *et al.*, "What is the fast Fourier transform?," *Proc. IEEE*, vol. 55, pp. 1664–1674, Oct. 1967.

[5] G. L. Rogers, "Experiments in diffraction microscopy," *Proc. Roy. Soc. Edinburgh, Sect. A*, vol. 63, pt. III, pp. 193–221, 1952.

[6] J. M. Smith and N. F. Moody, "Application of Fourier transforms in assessing the performance of an ultrasonic holography system," in *Acoustical Holography*, vol. I. New York: Plenum, 1969, ch. 6, pp. 97–112.

[7] A. Papoulis, *The Fourier Integral and Its Application*. New York: McGraw-Hill, 1962, p. 63.